# Numerical solutions of hyperbolic systems of conservation laws combining unsteady friction and viscoelastic pipes

Aboudou Seck

## ABSTRACT

The main contribution of the paper is to incorporate pipe-wall viscoelastic and unsteady friction in the derivation of the water-hammer solutions of non-conservative hyperbolic systems with conserved quantities as variables. The system is solved using the Godunov finite volume scheme to obtain numerical solutions. This results in the appearance of a new term in the mass conservation equation of the classical governing system. This new numerical algorithm implements the Godunov approach to one-dimensional hyperbolic systems of conservation laws on a finite volume stencil. The viscoelastic pipe-wall response in the mass conservation part of the source term has been modeled using generalized Kelvin–Voigt theory. For the momentum part of the source term a fast, robust and accurate numerical scheme linked to the Lambert *W*-function for calculating the friction factor has been used. A case study has been used to illustrate the influence of the various formulations; a comparison between the classical solution, the numerical solution including quasi-steady friction, the numerical solution incorporating the viscoelastic effects, and measurements are presented. The inclusion of viscoelastic effects results in better agreement between the measured and solved values.

**Key words** | finite volume, Godunov scheme, hydraulic transients, Riemann problem, viscoelastic pipe-wall, water-hammer

**Aboudou Seck**
Department of Civil Engineering Technology,
CÉGEP de Saint-Hyacinthe,
Saint-Hyacinthe, Quebec,
Canada
E-mail: *aseck@cegepsth.qc.ca*

## HIGHLIGHTS

- Incorporate the viscoelastic pipe and unsteady friction in water-hammer formulations.
- Present the solutions of non-conservative hyperbolic systems with conserved quantities as variables.
- Adapt the finite volume approach, which was developed for hyperbolic equations to tackle systems that are not in 'proper' conservation form.
- Give a new numerical algorithm in finite volume for study several variants.



doi: 10.2166/hydro.2020.119

## NOMENCLATURE

The following notation is used in this contribution.

### Variables and operators

| | |
|---|---|
| $a_0$ | Celerity of the pressure waves |
| $\mathbf{A}$ | Jacobian matrix of $\mathbf{F}$ respecting to $\mathbf{U}$ |
| $A_0$ | Cross-sectional pipe area |
| $c_1$ | Dimensionless parameter |
| $d$ | (operator) Differential |
| $D$ | Diameter of the pipe |
| $e$ | Pipe wall width |
| $E$ | Young's modulus of the pipe material |
| $E_k$ | Modulus of the spring of $k$-element elasticity |
| $E_V$ | Bulk modulus of elasticity |
| $\mathbf{F}$ | Vector flux in the $x$-direction |
| $f_q$ | Quasi-steady part of the friction factor |
| g | Gravitational acceleration |
| H | Piezometric head |
| $J_k$ | Creep-compliance of the spring of Kelvin–Voigt $k$-element |
| $k_S$ | Absolute roughness of pipe |
| $N$ | Cells number in the computational domain |
| $p$ | Pressure |
| $Q$ | Volume discharge |
| $Q_m$ | Mass discharge |
| $R$ | Pipe radius |
| $R_e$ | Reynolds number |
| S | Vector source term |
| t | Time |
| U | Vector variable |
| $V$ | Longitudinal fluid velocity |
| $x$ | Unit vector in the $x$-direction |
| $\Delta t$ | Calculation time step |
| $\Delta t_{\mathrm{Max}}$ | Maximum tolerable calculation time step |
| $\Delta t_{\mathrm{Max,S}}$ | Maximum tolerable calculation time step for stability of the discretized source term |
| $\Delta x$ | Cell size in $x$-direction |
| $\sigma$ | Stress |
| $\varepsilon$ | Total strain |
| $\varepsilon_e$ | Elastic strain |
| $\varepsilon_r$ | Retarded viscoelastic strain |
| $\lambda$ | Constant eigenvalue of the Jacobian matrix $\mathbf{A}$ |
| $\mu$ | Mass of fluid per unit length of pipe |
| $\rho$ | Mass density |
| $\tau_k$ | Retardation time of the dashpot of $k$-element |
| $\nu$ | Poisson's ratio |
| $v_r$ | Transverse velocity |
| $v_R$ | Radial velocity |
| $n, x$ | Solution obtained at $n$ after the solution of the conservation part in the $x$-direction |
| $n+1/2$ | Average value between $n$ and $n+1$ |

### Sub-script

| | |
|---|---|
| $b$ | Value to be prescribed at a boundary |
| $b, L$ | Value to be prescribed at the left boundary |
| $b, R$ | Value to be prescribed at the right boundary |
| $i$ | Cell number |
| $n$ | Time level |
| $n, x$ | Solution obtained at $n$ after the solution of the conservation part in the $x$-direction |
| $n+1/2$ | Average value between $n$ and $n+1$ |

## INTRODUCTION

In the detailed design of pipeline systems, water-hammer analysis is very important to select pipe characteristics and to specify surge control to prevent and/or mitigate any excessive pressures. The detailed design further attempts to elaborate the complete system response using various tools such as numerical modeling. Adamkowski & Lewandowski (2006) and Shamloo *et al.* (2015) reviewed a quasi-steady and four unsteady friction formulations (Zielke 1968; Trikha 1975; Brunone *et al.* 1991; Vardy & Brown 2003) for transient pipe flow. The Trikha (1975) model gives the Zielke (1968) model with assumptions that simplify the scheme. Bousso & Fuamba (2013) have numerically represented the unsteady friction in transient two-phase flow. Other unsteady friction

alternatives have been proposed by other authors (Zidouh *et al.* 2009; Weinerowska-Bords 2015). Their contribution bridges the gap between the detailed phase and the general concept but cannot be used as a full purpose tool for transient analysis since certain key parameters such as the effects of the viscoelastic pipe-wall are not incorporated.

Bergant *et al.* (2008a, 2008b) have experimentally studied key criteria that influence the pressure profile predicted by the water-hammer phenomenon. In general, numerical simulation tools assume that the friction factor is considered steady, quasi-steady, or dynamic; this has the tendency to overestimate the water-hammer peak pressures since the primary mechanism that may significantly affect pressure waveforms is the viscoelastic of the non-steel pipe-wall. In materials with viscous and elastic properties, the mechanical damping of the pressure response is larger than the damping phenomenon due to the fluid friction during the event of transient occurrences (Gally *et al.* 1979; Rieutord & Blanchard 1979; Rieutord 1982; Franke 1983; Güney 1983; Suo & Wylie 1990; Covas *et al.* 2004, 2005). Ferrante & Capponi (2018) have compared viscoelastic models with a different number of parameters for transient simulations.

The Godunov method is a conservative numerical scheme for solving PDE in CFD. This well-known conservative finite-volume approach computes a relative or exact Riemann solver at each cell. It is first-order accuracy in both time and space. This framework has been used in several papers to design first-order quasi-linear numerical methods in one-dimensional non-conservative hyperbolic systems, in the finite volume framework; see for example, Muñoz-Ruiz & Parés (2007), Guinot (2002a, 2002b, 2004), Bousso & Fuamba (2013), and Seck *et al.* (2017). Guinot (2003) focused on the scheme of the Godunov method to solve the classical water-hammer equations using finite volumes with steady friction. Pal *et al.* (2020) compared the first- and second-order FVMs based on the Godunov scheme with the method of characteristics (MOCs) and experimental water-hammer measurements available in the literature. Seck *et al.* (2017) developed the derivation of water-hammer formulations' hyperbolic systems of conservation laws with unsteady friction, which are not applicable for viscoelastic pipes because their non-negligible effects have not been taken into account.

Derived from the principles of conservation of momentum and mass, the water-hammer equations integrating unsteady friction and viscoelastic pipe-wall are expressed in hyperbolic systems of conservation laws with conserved quantities as variables. The presence of the viscoelastic pipe-wall terms preclude presentation in the integral (conservation) form and cause a source term to appear. The hyperbolic systems admit weak solutions in the form of discontinuities or 'shocks'. The treatment of these discontinuities requires special treatment of the flux function to avoid spurious oscillations.

The innovative components of this contribution are to present the water-hammer derivation equations with the effects of viscoelastic pipe-wall and unsteady friction, and adapt the finite volume approach with conserved variables, for hyperbolic equations of conservation laws. The aim of this contribution is to provide a new user-friendly complete numerical algorithm in finite volume for studying several variants or design water-hammer, in a short period, of the series of different characteristics of viscoelastic pipes in the distribution network that can be of benefit to engineers.

## METHODOLOGY

This paper focuses on implementation of the Godunov approach to the hyperbolic systems in one-dimensional conservation laws that describe the phenomenon of water-hammer integrating the viscoelastic pipe-wall and unsteady friction. The solution of a hyperbolic system of conservation laws by Godunov-type algorithms comprises six steps:

(i) discretization of space in finite volumes,
(ii) construction of generalised Riemann problems (GRP) at the cell,
(iii) conversion of the GRP into equivalent Riemann problems (ERP),
(iv) solution of the ERP,
(v) balance over the cells,
(vi) incorporation of the effect of the source terms.

The computation of the fluxes is detailed followed by a description of the complete numerical algorithm. A case study is examined with comparisons being made between

the numerical solution with quasi-steady friction, the numerical solution with viscoelastic pipe-wall, a classical solution, and the experimental results.

## Derivation from the conservation of mass and momentum

For constant pipe cross-section, the one-dimensional equations of water-hammer incorporating unsteady friction presented in vector form (Seck *et al.* 2017) are:

$$\frac{\partial \mathbf{U}}{\partial t}+\frac{\partial \mathbf{F}}{\partial x}=-\mathbf{R}\frac{\partial \mathbf{U}}{\partial x}+\mathbf{S}$$
$$\mathbf{U}=\begin{bmatrix}\mu\\ Q_m\end{bmatrix},\ \mathbf{F}=\begin{bmatrix}Q_m\\ A_0p\end{bmatrix},\ \boldsymbol{R}=ka_0\psi\begin{bmatrix}0 & 0\\ -V & 1\end{bmatrix},\ \mathbf{S}=\begin{bmatrix}0\\ -f_q|V|V\end{bmatrix} \tag{1}$$

where $\psi$ is expressed as:

$$\psi=\begin{cases}+1\ if\ V\dfrac{\partial V}{\partial x}>0\\ -1\ if\ V\dfrac{\partial V}{\partial x}<0\end{cases} \tag{2}$$

$k=\dfrac{\sqrt{C*}D}{2\mu+\sqrt{C*}D}$, $\mathbf{U}$ is the flow conserved variable vector, $\mathbf{F}$ the flux vector, $\mathbf{S}$ the source term vector, $D$ the inner pipe diameter (m), $C*$ the Vardy's shear decay constant related to the flow regime, $x$ the unit vector in $x$-direction, $t$ the time (s), $\mu=\rho A_0$ *is* the mass of liquid per unit length of pipe (kg/m), $Q_m=\mu V=\rho A_0 V$ the mass discharge (kg/s), $\rho$ the fluid density (kg/m$^3$), $A_0$ the cross-sectional pipe area (m$^2$), $V$ the longitudinal fluid velocity (m/s), $a_0$ wave speed (m/s), $f_q$ the steady state friction coefficient, and $p$ the pressure (Pa) where the formula will be given later (Equation (21)).

In the definitions and basic notion of conservation laws, the source term $\mathbf{S}$ can be a function of time $t$, space coordinate $x$ and flow variable vector U, combined or separately. In this form (Equation (1)), where only the conservation part remains on the left, the term $-\mathbf{R}\partial\mathbf{U}/\partial x$ on the right is considered as being part of the source term. This source term thus contains an additional term $-\mathbf{R}\partial\mathbf{U}/\partial x$. $\mathbf{S}$ is referred to as a hyperbolic source term, if it incorporates the derivative $\partial\mathbf{U}/\partial x$. Systems that can be written under the form of Equation (1) are also called systems of conservation laws with source term, or hyperbolic systems of conservation laws, or balance laws (Parés 2006). The incorporation of the unsteady friction results in the appearance of the quasilinear term $\mathbf{R}\partial\mathbf{U}/\partial x$ in the hyperbolic system (Equation (1)) thus destroying the classical integral form of the equations (Seck *et al.* 2018).

For turbulent flow, and laminar flow, $f_q$ in Equation (1) may be obtained, respectively, by the Colebrook–White formula and the Hagen–Poiseuille formula which are well-known and documented worldwide. If the flow is turbulent, the momentum part of the source term contains an implicit expression $f_q$ for the steady friction factor. Clamond (2009) has proposed a robust, accurate, and fast numerical scheme for calculating the Colebrook–White formula that is more efficient than the result regarding the Lambert $W$-function, also sometimes called the Omega (Corless *et al.* 1996, 1997) or simple approach such as the Haaland (1983) equation:

$$\frac{1}{\sqrt{f_q}}=\frac{2}{\ell}\cdot\varpi\left(\frac{\ell KR_e}{18.574};\ \ln\left(\frac{\ell R_e}{5.02}\right)\right) \tag{3}$$

where $K=k_S/D$ is equivalent absolute roughness $k_S$ divided by the pipe diameter $D$, $\ell=\ln 10\approx 2.302585093$ and $R_e$ the Reynolds number. The $\varpi$-function is linked to the Lambert $W$-function as:

$$\left.\begin{aligned}\varpi(x_1;x_2)&=W(\exp(x_1+x_2))-x_1\\ W(x)&\approx\ln(x)-\ln(\ln(x))\end{aligned}\right\} \tag{4}$$

To compute the steady state friction factor, Equation (3) can be rewritten as:

$$\frac{1}{\sqrt{f_q}}=\frac{2}{\ell}\cdot\left\{\ln\left(\frac{\ell R_e}{5.02}\right)-\ln\left[\frac{\ell KR_e}{18.574}+\ln\left(\frac{\ell R_e}{5.02}\right)\right]\right\} \tag{5}$$

where $\varpi$-function has been replaced with Lambert $W$-function for the sake of simplicity.

## The viscoelastic pipe-wall inclusion

In viscoelastic pipe-wall, the full strain $\varepsilon$ is divided into the sum of the retarded strain $\varepsilon_r$ and elastic strain $\varepsilon_e$ (Covas *et al.* 2004, 2005; Weinerowska-Bords 2006; Bergant *et al.* 2008a, 2008b):

$$\varepsilon = \varepsilon_e + \varepsilon_r \tag{6}$$

The elastic strain is introduced in the wave celerity expressed as:

$$a_0 = \sqrt{\frac{E_V/\rho}{1 + c_1 \dfrac{DE_V}{eE_0}}} \tag{7}$$

where $e$ is the pipe wall width, $E_V$ the fluid bulk modulus of elasticity (Pa), $E_0$ the pipe material Young's modulus (Pa), and $c_1$ is the constant that takes into account constraints and pipe cross-section dimensions; it is defined as (Streeter & Wylie 1993) for a thin-wall pipe fixed along its length.

$$c_1 = \frac{2e}{D}(1+\nu) + \frac{D}{D+e}(1-\nu^2) \tag{8}$$

in which, $\nu$ is the Poisson's ratio.

The viscoelastic influences only the continuity equation (Covas *et al.* 2004, 2005; Weinerowska-Bords 2006; Bergant *et al.* 2008a, 2008b).

The well-known and documented continuity equation that takes into consideration radial variations, for axisymmetric pipe flows, is given by:

$$\frac{\partial \rho}{\partial t} + \frac{\partial(\rho V)}{\partial x} + \frac{1}{r}\frac{\partial(\rho r v_r)}{\partial r} = 0 \tag{9}$$

in which $v_r$ is the transverse velocity (m/s) and $r$ the radial coordinate. By integrating that continuity Equation (9) along the pipe cross-sectional area,

$$\frac{\partial(A_0\rho)}{\partial t} + \frac{\partial(A_0\rho V)}{\partial x} + 2\pi\rho R v_R = 0 \tag{10}$$

where $v_R$ is the radial velocity at pipe-wall (m/s), $R$ the pipe radius. Rewritten as:

$$\frac{\partial \mu}{\partial t} + \frac{\partial Q_m}{\partial x} + \frac{2A_0\rho}{R} v_R = 0, \tag{11}$$

or

$$\frac{\partial \mu}{\partial t} + \frac{\partial Q_m}{\partial x} + \frac{4\mu}{D} v_R = 0 \tag{12}$$

The relationship between $v_R$ and pipe radial expansion is given by (Güney 1983; Duan *et al.* 2010; Chaudhry 2014):

$$v_R(x,t) = \frac{1}{2}\frac{\partial D}{\partial t} \text{ and } \frac{1}{\mathrm{D}}\frac{\partial D}{\partial t} = \frac{\partial \varepsilon}{\partial t} \tag{13}$$

From Equation (6),

$$\frac{\partial \varepsilon}{\partial t} = \frac{\partial(\varepsilon_e + \varepsilon_r)}{\partial t} \tag{14}$$

where $\partial\varepsilon_e/\partial t = 0$. It is a well-known fact that:

$$\frac{\partial \varepsilon}{\partial t} = \frac{\partial \varepsilon_r}{\partial t} \tag{15}$$

From Equations (12)–(14), the continuity Equation (9) can be finally rewritten:

$$\frac{\partial \mu}{\partial t} + \frac{\partial Q_m}{\partial x} + 2\mu\frac{d\varepsilon_r}{dt} = 0 \tag{16}$$

From a physical point of view, the third term in Equation (16) is the flux in the radial direction. That component is a function of conserved vector variable $\mu$, and time derivative of retarded strain $\varepsilon_r$, combined, but does not contain functions of any of derivatives of $\mu$.

Therefore, the general system incorporating the effects of viscoelastic pipe-wall (Equation (16)) and unsteady friction (Equation (1)) gives Equation (17) in terms of the 'conserved' dependent variables $\mu$ and $Q_m$:

$$\begin{cases} \dfrac{\partial \mu}{\partial t} + \dfrac{\partial Q_m}{\partial x} = -2\mu\dfrac{d\varepsilon_r}{dt} \\ \dfrac{\partial Q_m}{\partial t} + \dfrac{\partial}{\partial x}(A_0 p) = ka_0\psi\left(V\dfrac{\partial \mu}{\partial x} - \dfrac{\partial Q_m}{\partial x}\right) - f_q|V|V \end{cases} \tag{17}$$

or, in vector form:

$$\frac{\partial \mathbf{U}}{\partial \mathrm{t}}+\frac{\partial \mathbf{F}}{\partial \mathrm{x}}=-\mathbf{R}\frac{\partial \mathbf{U}}{\partial \mathrm{x}}+\mathbf{S}$$
$$\mathbf{U}=\begin{bmatrix}\mu\\ Q_m\end{bmatrix},\ \mathbf{F}=\begin{bmatrix}Q_m\\ A_0p\end{bmatrix},\ \mathbf{R}=ka_0\psi\begin{bmatrix}0 & 0\\ -V & 1\end{bmatrix},\ \mathbf{S}=\begin{bmatrix}-2\mu\dfrac{d\varepsilon_r}{dt}\\ -f_q|V|V\end{bmatrix} \tag{18}$$

The viscoelastic influences only the conservation of mass equation while the unsteady friction affects only the momentum. In viscoelastic materials (PVC, PE), the mechanical damping of the pressure response is larger than the damping phenomena due to the fluid friction during the event of transient occurrences (Gally *et al.* 1979; Rieutord & Blanchard 1979; Rieutord 1982; Franke 1983; Güney 1983; Suo & Wylie 1990; Covas *et al.* 2004, 2005). In fact, the primary mechanism that may seriously influence pressure waveforms is the viscoelastic of the non-steel pipe-wall (Bergant *et al.* 2008a, 2008b). Then, specifically for viscoelastic materials, the additional term quasilinear term $-\mathbf{R}\partial\mathbf{U}/\partial x$ contained in the source term can be neglected. Equation (18) may be rewritten as:

$$\left.\begin{array}{c}\dfrac{\partial \mathbf{U}}{\partial \mathrm{t}}+\dfrac{\partial \mathbf{F}}{\partial \mathrm{x}}=S\\ U=\begin{bmatrix}\mu\\ Q_m\end{bmatrix},\quad F=\begin{bmatrix}Q_m\\ A_0p\end{bmatrix},\quad S=\begin{bmatrix}-2\mu\dfrac{d\varepsilon_r}{dt}\\ -f_q|V|V\end{bmatrix}\end{array}\right\} \tag{19}$$

The integral form of that one-dimensional hyperbolic system Equation (19) may be expressed as follows:

$$\int_a^b[\mathbf{U}(x,t_2)-\mathbf{U}(x,t_1)]dx=-\int_{t_1}^{t_2}[\mathbf{F}(b,t)-\mathbf{F}(a,t)]dt+\int_{t_1}^{t_2}[\mathbf{S}(b,t)-\mathbf{S}(a,t)]dt \tag{20}$$

Equation (19) is equivalent to the Guinot's (2003) basic equation if viscoelastic pipe-wall is neglected. That inclusion of the viscoelastic pipe-wall results in the appearance of the term $-2\mu\dfrac{d\varepsilon_r}{dt}$ in the mass conservation part of the source term **S**. To close the vector Equation (19), the wave speed $a_0$ that also relate the variations of $\mu$ to those of the pressure $p$ is introduced as:

$$a_0=\left[\frac{d}{d\mu}(A_0p)\right]^{1/2} \tag{21}$$

where it is assumed that the wave speed depends on fluid compressibility, pipe physical characteristics, and external constraints.

Equation (19) may then be rewritten as:

$$\left.\begin{array}{c}\dfrac{\partial \mathbf{U}}{\partial t}+A\dfrac{\partial \mathbf{U}}{\partial x}=S\\ U=\begin{bmatrix}\mu\\ Q_m\end{bmatrix},\quad A=\begin{bmatrix}0 & 1\\ a_0^2 & 0\end{bmatrix},\quad S=\begin{bmatrix}-2\mu\dfrac{d\varepsilon_r}{dt}\\ -f_q|V|V\end{bmatrix}\end{array}\right\} \tag{22}$$

where $\mathbf{A}=\partial\mathbf{F}/\partial\mathbf{U}$ is the (constant) Jacobian matrix of the flux vector in $x$-direction with respect to the flow conserved variable vector. Since the homogeneous part of the system is linear, the two (constant) eigenvalues $\lambda^{(1)}$ and $\lambda^{(2)}$ of **A** are:

$$\left.\begin{array}{l}\lambda^{(1)}=-a_0\\ \lambda^{(2)}=+a_0\end{array}\right\} \tag{23}$$

The next section describes the solution process for the system.

## Numerical solution

Equation (19) is solved in two steps: like Seck *et al.* (2017), the first step uses the Guinot (2003) solution for the mass conservation part of the PDE omitting the right-hand part **S**:

$$\frac{\partial \mathbf{U}}{\partial t}+\frac{\partial \mathbf{F}}{\partial x}=0 \tag{24}$$

The second step uses Seck *et al.* (2017), Toro (2001), Guinot (2003), and Bousso & Fuamba (2013) treatment of the source term in (Equation (19)),

$$\frac{\partial \mathbf{U}}{\partial \mathrm{t}}=\mathbf{S} \tag{25}$$

The first-order time splitting is used. The viscoelastic model (based on the generalized Kelvin–Voigt application) in the mass conservation part of the source term is solved using the modified Covas *et al.* (2005) numerical scheme.

For the momentum part of the source term, the Colebrook–White equation is solved using a robust, fast, and accurate numerical scheme due to Clamond (2009).

## Solutions at the internal cells and at the boundaries

The conservation component omitting the source term **S** of Equation (19) is Equation (24). It is the same conservation component as in classical Guinot's (2003) equation. For the internal cells, Guinot (2003) constructs the Riemann problem $\mathbf{U}(x, t^n)$ and presents the solution $\mathbf{U}_{i+1/2}^{n+1/2}$ of this Riemann problem in Equation (26) computing the flux $\mathbf{F}_{i+1/2}^{n+1/2}$ between the time intervals $t^n$ and $t^{n+1}$ according to Equation (27).

$$\mathbf{U}_{i+1/2}^{n+1/2} = \begin{bmatrix} \mu_{i+1/2}^{n+1/2} \\ Q_{m,i+1/2}^{n+1/2} \end{bmatrix} = \frac{1}{2}\begin{bmatrix} \mu_i^n + \mu_{i+1}^n + (Q_{m,i}^n - Q_{m,i+1}^n)/a_0 \\ (\mu_i^n + \mu_{i+1}^n)a_0 + Q_{m,i}^n - Q_{m,i+1}^n \end{bmatrix} \tag{26}$$

$$\mathbf{F}_{i+1/2}^{n+1/2} = \mathbf{F}(\mathbf{U}_{i+1/2}^{n+1/2}) = \begin{bmatrix} Q_{m,i+1/2}^{n+1/2} \\ A_0 p_{i+1/2}^{n+1/2} \end{bmatrix} \tag{27}$$

where $p_{i+1/2}^{n+1/2} = p_{ref} + a_0^2(\mu_{i+1/2}^{n+1/2} - \mu_{ref})$ according to Equation (21); $p_{ref}$ is a reference pressure at which the density $\rho_{ref}$ is known. $\mu_{ref}$ is calculated as $\mu_{ref} = A_0\rho_{ref}$.

The flux solutions for a prescribed pressure $p_b$ boundary at the left side ($p_{b,L}$) and the right side ($p_{b,R}$) are, respectively, given by:

$$\mathbf{F}_{1/2}^{n+1/2} = \begin{bmatrix} Q_{m,1}^n + (\mu_{1/2}^{n+1/2} - \mu_1^n)a_0 \\ A_0 p_{b,L} \end{bmatrix} \tag{28}$$

$$\mathbf{F}_{N+1/2}^{n+1/2} = \begin{bmatrix} Q_{m,N}^n + (\mu_N^n - \mu_{N+1/2}^{n+1/2})a_0 \\ A_0 p_{b,R} \end{bmatrix} \tag{29}$$

In Equations (28) and (29), $p_b$ represents a pressure to be determined at the boundary. $\mu_{1/2}^{n+1/2}$ (at the left) and $\mu_{N+1/2}^{n+1/2}$ (at the right) is obtained from the prescribed pressure $p_b$ using:

$$\mu_b = \mu_{ref} + \frac{A_0}{a_0^2}(p_b - p_{ref}) \tag{30}$$

The fluxes for a prescribed discharge $Q_b$ at the left and at the right side boundary are, respectively, given by:

$$\mathbf{F}_{1/2}^{n+1/2} = \begin{bmatrix} Q_b\mu_{1/2}^{n+1/2}/A_0 \\ A_0 p_{1/2}^{n+1/2} \end{bmatrix} \tag{31}$$

$$\mathbf{F}_{N+1/2}^{n+1/2} = \begin{bmatrix} Q_b\mu_{N+1/2}^{n+1/2}/A_0 \\ A_0 p_{N+1/2}^{n+1/2} \end{bmatrix} \tag{32}$$

where $\mu_{1/2}^{n+1/2}$ in Equation (31) and $\mu_{N+1/2}^{n+1/2}$ in Equation (32) are obtained, respectively, from:

$$\mu_{1/2}^{n+1/2} = \frac{Q_{m,1}^n - a_0\mu_1^n}{\frac{Q_b}{A_0} - a_0} \tag{33}$$

$$\mu_{N+1/2}^{n+1/2} = \frac{Q_{m,N}^n + a_0\mu_N^n}{\frac{Q_b}{A_0} + a_0} \tag{34}$$

According to Equation (21), $p_{1/2}^{n+1/2}$ in Equation (31) and $p_{N+1/2}^{n+1/2}$ in Equation (32) are obtained, respectively, from:

$$p_{1/2}^{n+1/2} = A_0 p_{ref} + \left(\mu_{1/2}^{n+1/2} - \mu_{ref}\right)a_0^2 \tag{35}$$

$$p_{N+1/2}^{n+1/2} = A_0 p_{ref} + \left(\mu_{N+1/2}^{n+1/2} - \mu_{ref}\right)a_0^2 \tag{36}$$

For all cells, the balance is performed omitting the source term using:

$$\mathbf{U}_i^{n+1,x} = \mathbf{U}_i^n + \frac{\Delta t}{\Delta x_i}(\mathbf{F}_{i-1/2}^{n+1/2} - \mathbf{F}_{i+1/2}^{n+1/2}) \tag{37}$$

## Discretization of the source term

The first-order 'time-splitting', 'fractional steps' or 'Strang (1968) splitting' technique is used. Taking the provisional solution $\mathbf{U}_i^{n+1,x}$ obtained at the end of the Godunov step as a starting point, the final solution $\mathbf{U}_i^{n+1}$ of the source term at the end of the time step is presented by Toro (2001), Guinot (2003), Bousso & Fuamba (2013), and Seck *et al.* (2017) in the following form:

$$\mathbf{U}_i^{n+1} = \mathbf{U}_i^{n+1,x} + \mathbf{S}(\mathbf{U}_i^{n+1,x})\Delta t \tag{38}$$

where $\mathbf{S}(\mathbf{U}_i^{n+1,x})$ is the source term value, determined by using $\mathbf{U}_i^{n+1,x}$.

In the present example, the vector Equation (25) is equivalent to the system of ordinary differential equations (ODEs):

$$\left.\begin{aligned}\frac{d\mu}{dt} &= -2\mu\frac{d\varepsilon_r}{dt}\\ \frac{dQ_m}{dt} &= -f_q Q_m|Q_m|\end{aligned}\right\} \tag{39}$$

Generally, to perform the discretization of source term, two options are possible: i) the explicit method that can be applied for any expression of source term, and ii) an analytical method that is used here, owing to the simplicity of the expression of the particular source term. In the present example, the very simple expression of the source term allows an analytical solution to be derived. The independent ODEs Equation (39) has the following discretized form:

$$\left.\begin{aligned}\mu_i^{n+1} &= \mu_i^{n+1,x} exp(-2\varepsilon_{r,i}^{n+1})\\ Q_{m,i}^{n+1} &= \frac{Q_{m,i}^{n+1,x}}{1+|Q_{m,i}^{n+1,x}|\Delta t f_q}\end{aligned}\right\} \tag{40}$$

The creep-compliance function $J(t)$ at time $t$ must be known to calculate the time derivative of the retarded strain $\varepsilon_{r,i}^{n+1}$. The generalized Kelvin–Voigt model for a material with viscous and elastic properties, i.e., Equation (41) represented in Figure 1, is generally needed to characterize the function $J(t)$ of the creep-compliance (Aklonis *et al.* 1972; Gally *et al.* 1979; Suo & Wylie 1990; Covas *et al.* 2005):

$$J(t) = J_0 + \sum_{k=1}^{N} J_k(1 - e^{-t/\tau_k}) \tag{41}$$

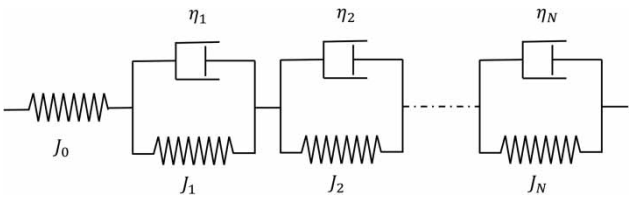


**Figure 1** | Generalized Kelvin–Voigt model of viscoelastic behavior of pipe hoop.

where $J_0 = 1/E_0$ is the creep-compliance of the initial spring ($Pa^{-1}$), $J_k = 1/E_k$ the creep-compliance of the spring ($Pa^{-1}$) of Kelvin–Voigt $k$-element, $E_k$ the modulus of elasticity (Pa) of the spring of $k$-element, $\tau_k = \eta_k/E_k$ the retardation time (s) of the dashpot of $k$-element.

The values of $J_k$ and $\tau_k$ were calibrated with the creep-compliance test details. The retarded viscoelastic strain $\varepsilon_{r,i}^{n+1}$ is computed as the addition of these parameters of individual Kelvin–Voigt element $k$ as:

$$\varepsilon_{r,i}^{n+1} = \sum_{k=1}^{N} \varepsilon_{rk,i}^{n+1} \tag{42}$$

Founded on the solving of the analytical differentiation equation of the integral form of the strain time-derivative, and after mathematical manipulations for each Kelvin–Voigt element $k$, Covas *et al.* (2005) proposed Equations (43)–(45), which are numerical approximations:

$$\frac{\partial\varepsilon_{rk}(x,t)}{\partial t} = \frac{J_k}{\tau_k}F(x,t) - \frac{\tilde{\varepsilon}_{rk}(x,t)}{\tau_k} \tag{43}$$

where the functions $F(x,t)$ and $\tilde{\varepsilon}_{rk}(x,t)$, respectively, are defined by:

$$F(x,t) = \frac{c_1 D}{2e}\rho g[H(x,t) - H_0(x)] \tag{44}$$

$$\begin{aligned}\tilde{\varepsilon}_{rk}(x,t) &= J_k F(x,t) - J_k e^{-\Delta t/\tau_k}F(x,t-\Delta t)\\ &\quad - J_k\tau_k(1-e^{-\Delta t/\tau_k})\frac{F(x,t)-F(x,t-\Delta t)}{\Delta t}\\ &\quad + e^{-\Delta t/\tau_k}\tilde{\varepsilon}_{rk}(x,t-\Delta t)\end{aligned} \tag{45}$$

where g is the gravitational acceleration and $H$ the piezometric head (m). If the pipe material is isotropic and homogeneous, the Poisson's ratio is constant and viscoelastic for small strains is linear; function $F(x,t)$ is equivalent to the stress $\sigma$ (Pa) for the pipe subjected to the internal pressure expressed as (Streeter & Wylie 1993):

$$\sigma = \frac{c_1 D}{2e}dp \tag{46}$$

Substituting Equation (21) into Equation (44) in conservative form, the function $F(x, t)$ can be rewritten as:

$$F(x, t) = \frac{c_1 D a_0^2}{2eA_0}[\mu(x, t) - \mu_{\text{ref}}] \tag{47}$$

The final discretization of the source term is:

$$\left.\begin{aligned} \mu_i^{n+1} &= \mu_i^{n+1,x} exp\left[-2\Delta t \sum_{k=1}^{N}\left(\frac{J_k}{\tau_k}F(x, t) - \frac{\tilde{\varepsilon}_{rk}(x, t)}{\tau_k}\right)\right] \\ Q_{m,i}^{n+1} &= \frac{Q_{m,i}^{n+1,x}}{1 + |Q_{m,i}^{n+1,x}|\Delta t f_q} \end{aligned}\right\} \tag{48}$$

On condition of a rigid pipe-wall, the exponential term tends to 1 in the solution of the mass conservation part of the source term **S**.

### Computational time step

For the computational time step, since the approach is non-implicit, the CFL condition for stability must be respected, i.e., the maximum permissible time step $\Delta t_{Max}$ (Guinot 2003) is as follows:

$$\Delta t_{\text{Max}} = \text{Min}\left[\min_{i=1,\ldots,N}\left(\frac{\Delta x_i}{a_0}\right); \Delta t_{\text{Max,S}}\right] \tag{49}$$

For the stability analysis of the discretized source term, the maximum tolerable calculation time step $\Delta t_{Max,S}$ is needed. It is given by:

$$\Delta t_{\text{Max,S}} = \min_{i=1,\ldots,N}\left[-2\frac{\mathbf{U}_i^{n+1,x}}{\mathbf{S}(\mathbf{U}_i^{n+1,x})}\right] \tag{50}$$

### Resolution algorithm

The user-friendly proposed algorithm is presented in Figure 2.

## RESULTS AND DISCUSSION

A case study has been simulated. Data from the experimental test conducted by Covas *et al.* (2004) have been compared with the numerical results.

### Experimental setup

The results of experimental studies conducted by Covas *et al.* (2004) obtained from a PE pipe-rig at Imperial College and considered to be of good quality are compared with the mathematical model. The experimental setup is composed of a 277 m long PE pipe with a thickness of 6.25 mm and an inner diameter of 50.6 mm that connects to an upstream air vessel. Initial steady flow ($Q_0 = 1.008$ l/s) are followed by a transient occurrence initiated by the sudden closure of a globe valve at the downstream end. $\rho_{ref} = 1{,}000$ kg/m$^3$ and g = 9.81 m/s$^2$. The initial wave celerity $a_0$ was evaluated at 395 m/s. The pressure waves were computed and compared with the corresponding experimental values at location #1 (distance $x = 273$ m from upstream), location #5 (distance $x = 117.5$ m from upstream) and location #8 (distance $x =$ 199 m from upstream). The values of the creep coefficients $J_k$ for the retardation times $\tau_k$ are specified as follows. A full description of the collected data and the experimental system may be found in Covas *et al.* (2004).

$J_0 = 0.7.10^{-9}$ Pa$^{-1}$
$J_1 = 0.1394.10^{-9}$ Pa$^{-1}$; $\tau_1 = 0.05$ s;
$J_2 = 0.0062.10^{-9}$ Pa$^{-1}$; $\tau_2 = 0.5$ s;
$J_3 = 0.1148.10^{-9}$ Pa$^{-1}$; $\tau_3 = 1.5$ s;
$J_4 = 0.3425.10^{-9}$ Pa$^{-1}$; $\tau_4 = 5$ s;
$J_5 = 0.0928.10^{-9}$ Pa$^{-1}$; $\tau_5 = 10$ s;

### Results and discussion

The water-hammer equations incorporating viscoelastic pipe-wall were solved using the Godunov scheme detailed above. In keeping with the objectives of this paper, results were obtained for the analytical solution, the numerical solution with quasi-steady friction, and the numerical solution including the tuned viscoelastic model using a time step of $\Delta t = 0.0008$ *s*. The experimental measurements are compared with these results. Good accord between measured and computed viscoelastic profiles has been obtained (Figures 3–5).

Comparison between the results indicates that the inclusion of viscoelasticity has a serious impact on the pressure profiles. The quasi-steady friction model does not reproduce the progression of the aspect of the pressure

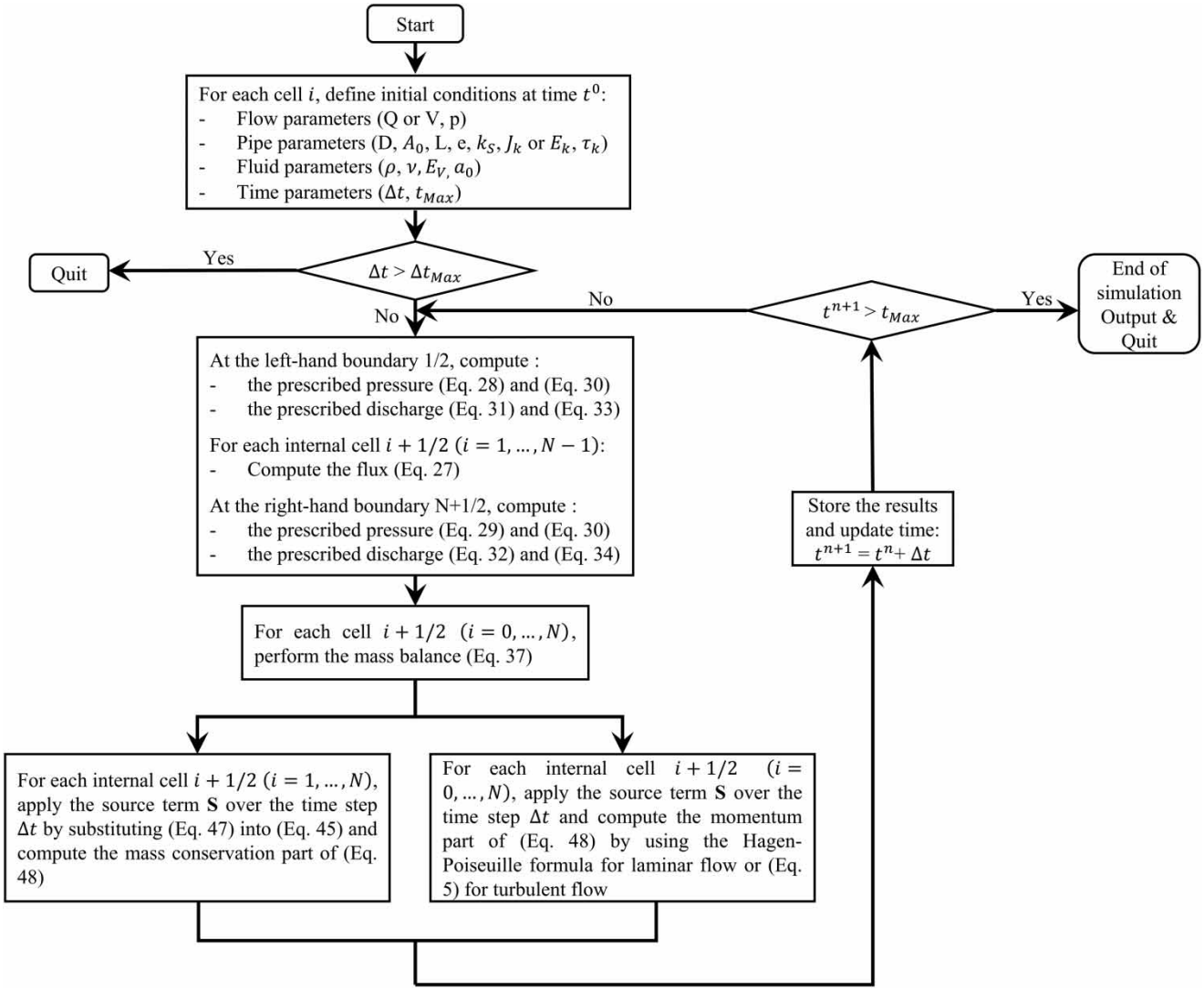


**Figure 2** | Schematic of the proposed algorithm.

waves very well. They also display phase shift errors. The quasi-steady friction model undervalues the propagation and damping predicted by the (physically) more accurate viscoelastic model which tends to attenuate the magnitude of the overpressures more rapidly. Due to damping, the waves will be of decreasing amplitude until the final equilibrium pressure is reached. In the present context given the simple geometry and non-varying fluid properties (the fluid is slightly compressible), the basic Godunov scheme is appropriate for the analysis of water-hammer phenomenon. The wave profile of the viscoelastic line is smooth and the wave fronts are smeared which justify the presence of a rarefaction wave. That front smearing is caused by the exponential term contained in the mass conservation equation (Equation (40)). The Godunov scheme introduces a non-negligible diffusion. This explains the use of a large number of calculation cells to obtain a quality solution similar to that of a higher order scheme that requires few computing cells. More cells and therefore more computational effort is required for one-order scheme. But, for a robust and fast one-order scheme that runs in a short time with many cells, the use of a higher order scheme is not justified, because it will only improve the solution just weakly.

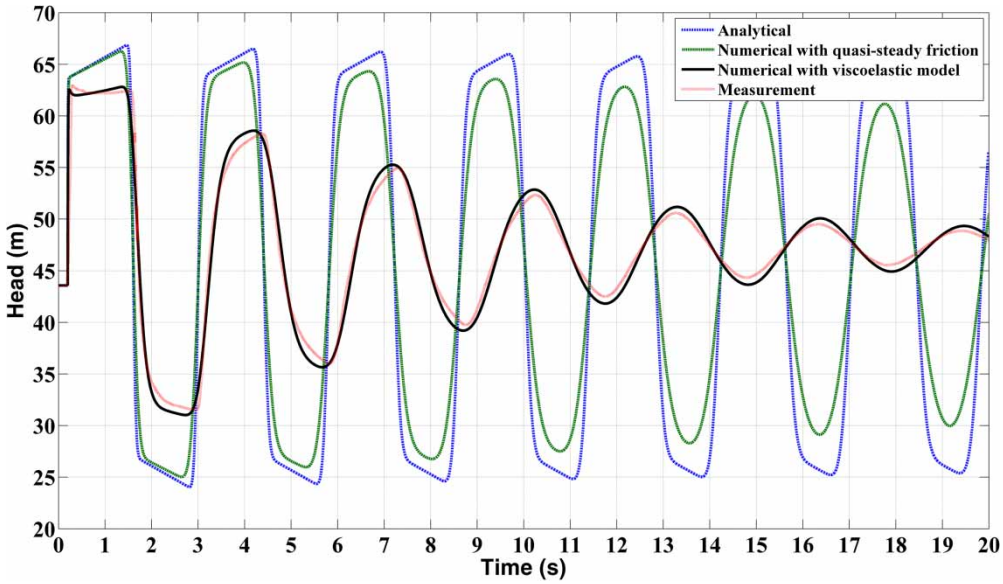


**Figure 3** | Pressure profiles ($\Delta t = 0.0008$ s, $N = 100$ cells) at location #1.

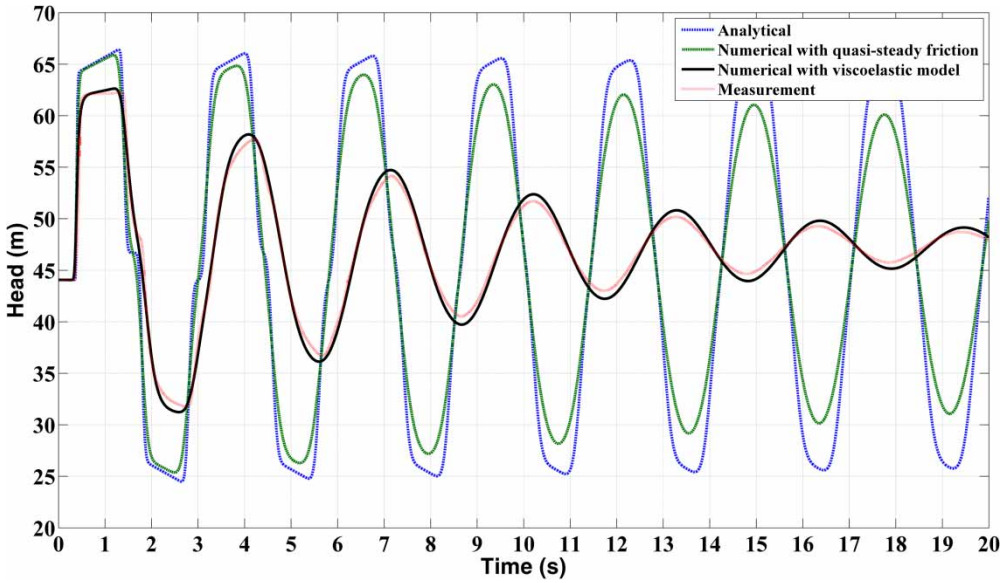


**Figure 4** | Pressure profiles ($\Delta t = 0.0008$ s, $N = 100$ cells) at location #8.

## CONCLUSIONS

The water-hammer equations, in conservation form, combining viscoelastic pipe-wall and unsteady friction, are developed and numerically solved using a finite volume formulation for engineering applications. A robust, simple, accurate, and fast computational algorithm based on the Godunov scheme for one-dimensional hyperbolic systems is presented in some detail. Incorporation of the viscoelastic pipe-wall results in the appearance of a new term in the mass conservation part of the source term in the hyperbolic system of governing partial differential

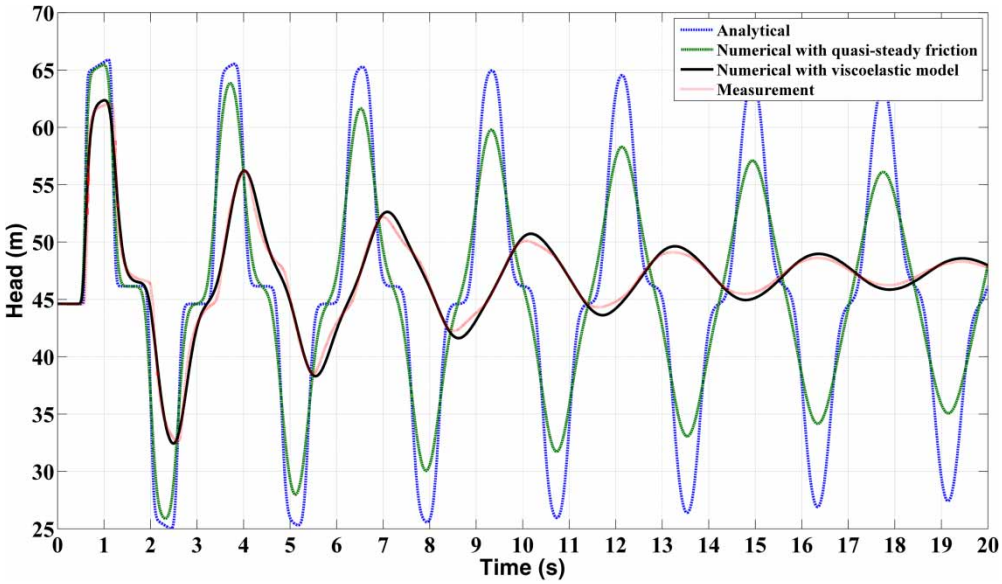


**Figure 5** | Pressure profiles ($\Delta t = 0.0008$ s, $N = 100$ cells) at location #5.

equations. From a physical point of view, this source term in mass conservation part is the flux in the radial direction. A case study has been presented to compare the separate impacts on wave attenuation with time. The findings indicate, as expected, inclusion of viscoelasticity reduces the peak water-hammer pressures. The model developed appears to be able to satisfactorily predict transient pressures in viscoelastic pipes and can be a useful tool for qualitative analysis.

These equations, as expected, admit 'weak' solutions with hydraulic jumps being the discontinuities. Using local first-order approximations to handle the spurious behavior near shocks does work without the expense of additional computational time. Computational time for the case studied took only 1 minute and 28 secs on a PC. Thus, for engineering applications, several variants for the design of series of different characteristic viscoelastic pipes in distribution networks may be studied in a short period of time with a spatial discretization not necessarily uniform.

The algorithm introduced in this paper could be used however, of course with some modifications, in the high-order schemes. This first-order proposed algorithm, in the context of hydraulic transients in pressurised pipelines incorporating viscoelastic pipe-wall and unsteady friction, is an interesting start to achieve this aim.

## DATA AVAILABILITY STATEMENT

All relevant data are included in the paper or its Supplementary Information.

## REFERENCES

Adamkowski, A. & Lewandowski, M. 2006 Experimental examination of unsteady friction models for transient pipe flow simulation. *Journal of Fluids Engineering* **128** (6), 1351–1363.

Aklonis, J., MacKnight, W. & Shen, M. 1972 *Introduction to Polymer Viscoelasticity*. Wiley, New York, USA, 481 p.

Bergant, A., Tijsseling, A. S., Vítkovský, J. P., Covas, D. I., Simpson, A. R. & Lambert, M. F. 2008a Parameters affecting water-hammer wave attenuation, shape and timing – part 1: mathematical tools. *Journal of Hydraulic Research* **46** (3), 373–381.

Bergant, A., Tijsseling, A. S., Vítkovský, J. P., Covas, D. I., Simpson, A. R. & Lambert, M. F. 2008b Parameters affecting water-hammer wave attenuation, shape and timing – part 2: case studies. *Journal of Hydraulic Research* **46** (3), 382–391.

Bousso, S. & Fuamba, M. 2013 Numerical simulation of unsteady friction in transient two-phase flow with Godunov method. *Journal of Water Resource and Protection* **5** (11), 1048.

Brunone, B., Golia, U. & Greco, M. 1991 Modelling of fast transients by numerical methods. In *Proceedings of the International Conference on Hydraulic Transients with Water Column Separation*, 4–6 September, Valencia, Spain, pp. 273–280.

Chaudhry, M. H. 2014 *Applied Hydraulic Transients*. Springer, New York, USA.

Clamond, D. 2009 Efficient resolution of the colebrook equation. *Industrial & Engineering Chemistry Research* **48** (7), 3665–3671.

Corless, R. M., Gonnet, G. H., Hare, D. E., Jeffrey, D. J. & Knuth, D. E. 1996 On the LambertW function. *Advances in Computational Mathematics* **5** (1), 329–359.

Corless, R. M., Jeffrey, D. J. & Knuth, D. E. 1997 A sequence of series for the Lambert W function. In *Proceedings of the 1997 International Symposium on Symbolic and Algebraic Computation*, 21–23 July, Maui, Hawaii, USA.

Covas, D., Stoianov, I., Ramos, H., Graham, N. & Maksimovic, C. 2004 The dynamic effect of pipe-wall viscoelasticity in hydraulic transients. part I – experimental analysis and creep characterization. *Journal of Hydraulic Research* **42** (5), 517–532.

Covas, D., Stoianov, I., Mano, J. F., Ramos, H., Graham, N. & Maksimovic, C. 2005 The dynamic effect of pipe-wall viscoelasticity in hydraulic transients. part II – model development, calibration and verification. *Journal of Hydraulic Research* **43** (1), 56–70.

Duan, H.-F., Ghidaoui, M., Lee, P. J. & Tung, Y.-K. 2010 Unsteady friction and visco-elasticity in pipe fluid transients. *Journal of Hydraulic Research* **48** (3), 354–362.

Ferrante, M. & Capponi, C. 2018 Comparison of viscoelastic models with a different number of parameters for transient simulations. *Journal of Hydroinformatics* **20** (1), 1–17.

Franke, P.-G. 1983 Computation of unsteady pipe flow with respect to visco-elastic material properties. *Journal of Hydraulic Research* **21** (5), 345–353.

Gally, M., Guney, M. & Rieutord, E. 1979 An investigation of pressure transients in viscoelastic pipes. *Journal of Fluids Engineering* **101** (4), 495–499.

Guinot, V. 2002a The time-line interpolation method for large-time-step Godunov-type schemes. *Journal of Computational Physics* **177** (2), 394–417.

Guinot, V. 2002b An unconditionally stable, explicit Godunov scheme for systems of conservation laws. *International Journal for Numerical Methods in Fluids* **38** (6), 567–588.

Guinot, V. 2003 *Godunov-type Schemes: An Introduction for Engineers*. Elsevier Science, Amsterdam, The Netherlands.

Guinot, V. 2004 High resolution Godunov-type schemes with small stencils. *International Journal for Numerical Methods in Fluids* **44** (10), 1119–1162.

Güney, M. 1983 Waterhammer in viscoelastic pipes where cross-section parameters are time-dependent. *Fourth International Conference on Pressure Surges*, September, Bath, UK.

Haaland, S. E. 1983 Simple and explicit formulas for the friction factor in turbulent pipe flow. *Journal of Fluids Engineering* **105** (1), 89–90.

Muñoz-Ruiz, M. L. & Parés, C. 2007 Godunov method for conservative hyperbolic systems. *ESAIM: Mathematical Modelling and Numerical Analysis-Modélisation Mathématique et Analyse Numérique* **41** (1), 169–185.

Pal, S., Hanmaiahgari, P. R. & Lambert, M. F. 2020 Efficient approach toward the application of godunov method to hydraulic transients. *Journal of Hydroinformatics* **22**, 1370–1390.

Parés, C. 2006 Numerical methods for nonconservative hyperbolic systems: a theoretical framework. *SIAM Journal on Numerical Analysis* **44** (1), 300–321.

Rieutord, E. 1982 Transient response of fluid viscoelastic lines. *Journal of Fluids Engineering* **104** (3), 335–341.

Rieutord, E. & Blanchard, A. 1979 Ecoulement non-permanent en conduite viscoelastique – coup de bélier. *Journal of Hydraulic Research, IAHR* **17** (1), 217–229.

Seck, A., Fuamba, M. & Kahawita, R. 2017 Finite-volume solutions to the water-hammer equations in conservation form incorporating dynamic friction using the Godunov scheme. *Journal of Hydraulic Engineering* **143** (9), 04017029.

Seck, A., Fuamba, M. & Kahawita, R. 2018 Closure to 'Finite-volume solutions to the water-hammer equations in conservation form incorporating dynamic friction using the Godunov scheme' by Aboudou Seck, Musandji Fuamba, and René Kahawita. *Journal of Hydraulic Engineering* **145** (2), 07018023.

Shamloo, H., Norooz, R. & Mousavifard, M. 2015 A review of one-dimensional unsteady friction models for transient pipe flow. *Cumhuriyet Science Journal* **36** (3), 2278–2288.

Strang, G. 1968 On the construction and comparison of difference schemes. *SIAM Journal on Numerical Aanalysis* **5** (3), 506–517.

Streeter, V. L. & Wylie, E. B. 1993 *Fluid Transients in Systems*. Prentice-Hall, Englewood Cliffs, NJ, USA.

Suo, L. & Wylie, E. 1990 Complex wavespeed and hydraulic transients in viscoelastic pipes. *Journal of Fluids Engineering* **112** (4), 496–500.

Toro, E. F. 2001 *Shock-capturing Methods for Free-Surface Sshallow Flows*. John Wiley & Sons, Chichester, UK.

Trikha, A. K. 1975 An efficient method for simulating frequency-dependent friction in transient liquid flow. *Journal of Fluids Engineering* **97** (1), 97–105.

Vardy, A. & Brown, J. 2003 Transient turbulent friction in smooth pipe flows. *Journal of Sound and Vibration* **259** (5), 1011–1036.

Weinerowska-Bords, K. 2006 Viscoelastic model of waterhammer in single pipeline-problems and questions. *Archives of Hydro-Engineering and Environmental Mechanics* **53** (4), 331–351.

Weinerowska-Bords, K. 2015 Alternative approach to convolution term of viscoelasticity in equations of unsteady pipe flow. *Journal of Fluids Engineering* **137** (5), 054501.

Zidouh, H., Labraga, L. & William-Louis, M. 2009 Unsteady wall shear stress in transient flow using electrochemical method. *Journal of Fluids Engineering* **131** (5), 051403.

Zielke, W. 1968 Frequency-dependent friction in transient pipe flow. *Journal of Basic Engineering* **90** (1), 109–115.

First received 22 July 2020; accepted in revised form 29 September 2020. Available online 3 November 2020